Supporting Information

Thomas et al. 10.1073/pnas.1308115110

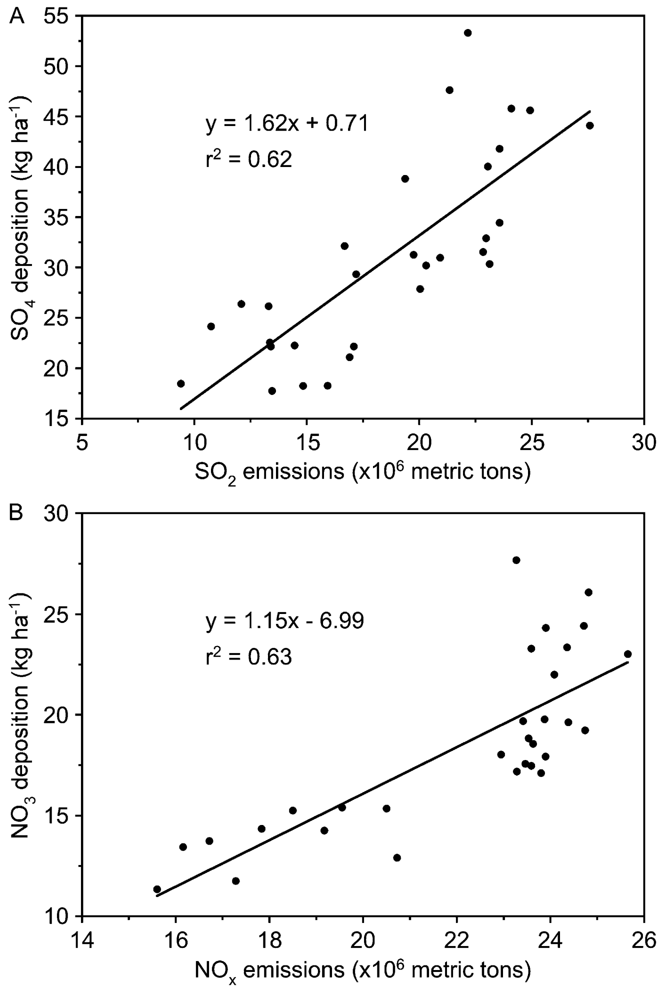

Fig. S1. (*A*) The relationship between estimates of US SO_2 emissions (million metric tons) and SO_4 deposition (kg·ha^{-1}) between 1979 and 2008. (*B*) The relationship between US NO_x emissions (million metric tons) and NO_3 deposition (kg·ha^{-1}) between 1979 and 2008. Both SO_4 and NO_3 are wet deposition measurements from the National Atmospheric Deposition Program Monitoring Location, Parsons WV18, Tucker County, WV, which began in 1979 (1). US SO_2 emissions are taken from refs. 2 and 3.

1. National Atmospheric Deposition Program (NRSP-3) 2013. NADP Program Office, Illinois State Water Survey. Available at http://nadp.sws.uiuc.edu/sites/siteinfo.asp?net=NTN&id=WV18.
2. Lefohn AS, Husar JD, Husar RB (1999) Estimating historical anthropogenic global sulfur emission patterns for the period 1850–1990. *Atmos Environ* 33(21):3435–3444.
3. US Environmental Protection Agency (2012) National Emissions Inventory (NEI) Air Pollution Emissions. Available: www.epa.gov/ttn/chief/trends/index.html. Accessed September 8, 2012.

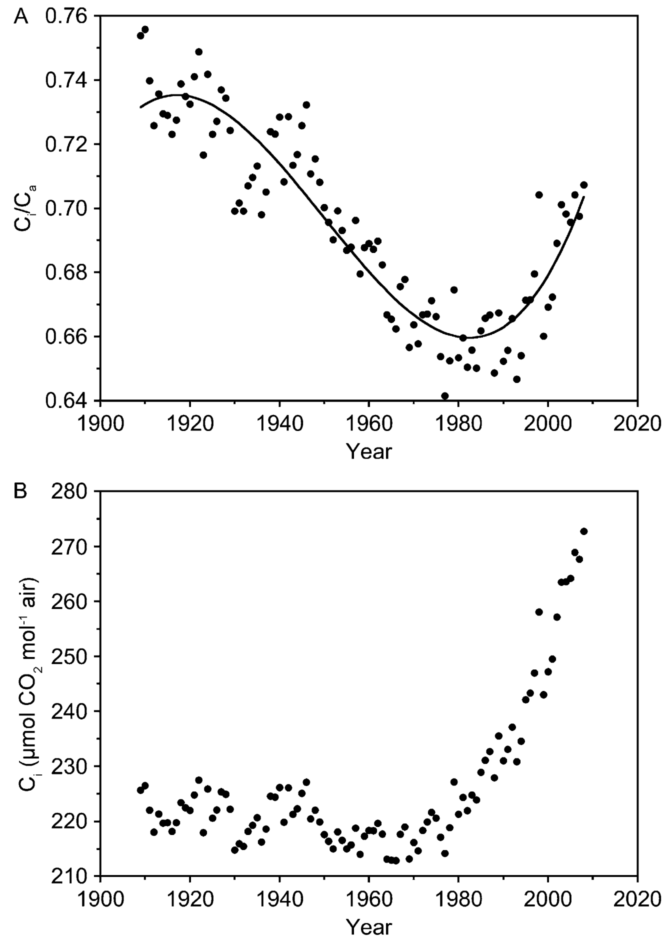

Fig. S2. Temporal trends of (*A*) the ratio of internal leaf CO_2 concentration to atmospheric CO_2 concentration. (C_i/C_a) derived from Δ^{13}C from tree rings of *Juniperus virginiana* and (*B*) C_i derived from C_i/C_a and C_a. Values of C_a were taken from refs. 1 and 2.

1. Etheridge DM, et al. (1998) Historical CO_2 records from the Law Dome DE08, DE08-2, and DSS ice cores. *Trends: A Compendium of Data on Global Change* (Carbon Dioxide Information Analysis Center, Oak Ridge National Laboratory, US Department of Energy, Oak Ridge, TN). Available at http://cdiac.ornl.gov/trends/co2/lawdome.html.
2. Keeling RF, Piper SC, Bollenbacher AF, Walker JS (2009) Atmospheric CO_2 records from sites in the SIO air sampling network, in *Trends: A Compendium of Data on Global Change* (Carbon Dioxide Information Analysis Center, Oak Ridge National Laboratory, US Department of Energy, Oak Ridge, TN). Available at http://cdiac.ornl.gov/trends/co2/sio-mlo.html.

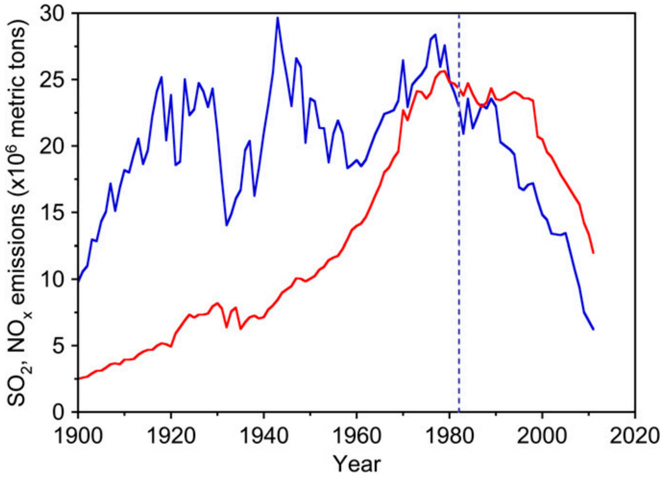

Fig. S3. Temporal trends of US emissions of sulfur dioxide (blue line) and nitrogen oxides (red line) (1, 2). The vertical dotted blue line at 1982 represents the year predicted from a third-order polynomial where the shift in $\Delta^{13}C$ occurs in the *Juniperus virginiana* tree rings (Fig. 2*B*).

1. Lefohn AS, Husar JD, Husar RB (1999) Estimating historical anthropogenic global sulfur emission patterns for the period 1850-1990. *Atmos Environ* 33(21):3435–3444.
2. US Environmental Protection Agency (2012) *National Emissions Inventory (NEI) Air Pollution Emissions* (US Environmental Protection Agency, Chicago). Available at www.epa.gov/ttn/chief/trends/index.html. Accessed September 8, 2012.

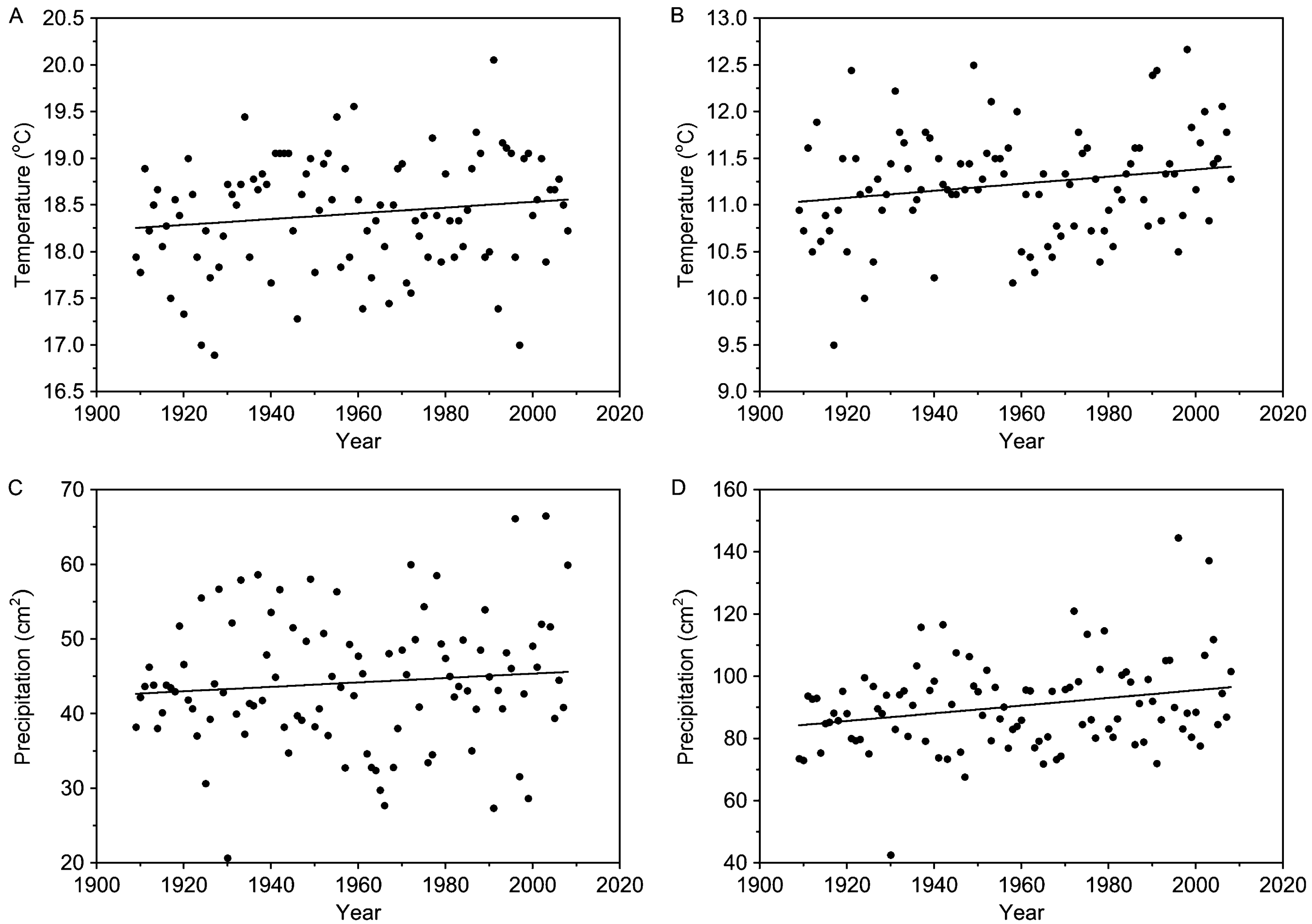

Fig. S4. Temporal trends in climate factors, including (*A*) growing season temperature ($y = 0.003x + 12.35$; $r^2 = 0.022$, $P < 0.142$), (*B*) yearly temperature ($y = 0.004x + 3.80$; $r^2 = 0.037$, $P < 0.057$), (*C*) growing season precipitation ($y = 0.030x - 14.55$; $r^2 = 0.010$, $P < 0.315$), and (*D*) yearly precipitation ($y = 0.124x - 151.56$; $r^2 = 0.063$, $P < 0.012$). Climate data are from West Virginia District 6, which is the region that contains the *J. virginiana* stand in this study (1).

1. National Oceanic and Atmospheric Administration (NOAA) National Climatic Data Center (2012) *West Virginia Climate Region 6 Meteorological Data 1895–2009* (NOAA, Asheville, NC). Available at www.ncdc.noaa.gov/temp-and-precip/time-series/index.php?parameter=tmp&month=4&year=2008&filter=12&state=46&div=6.

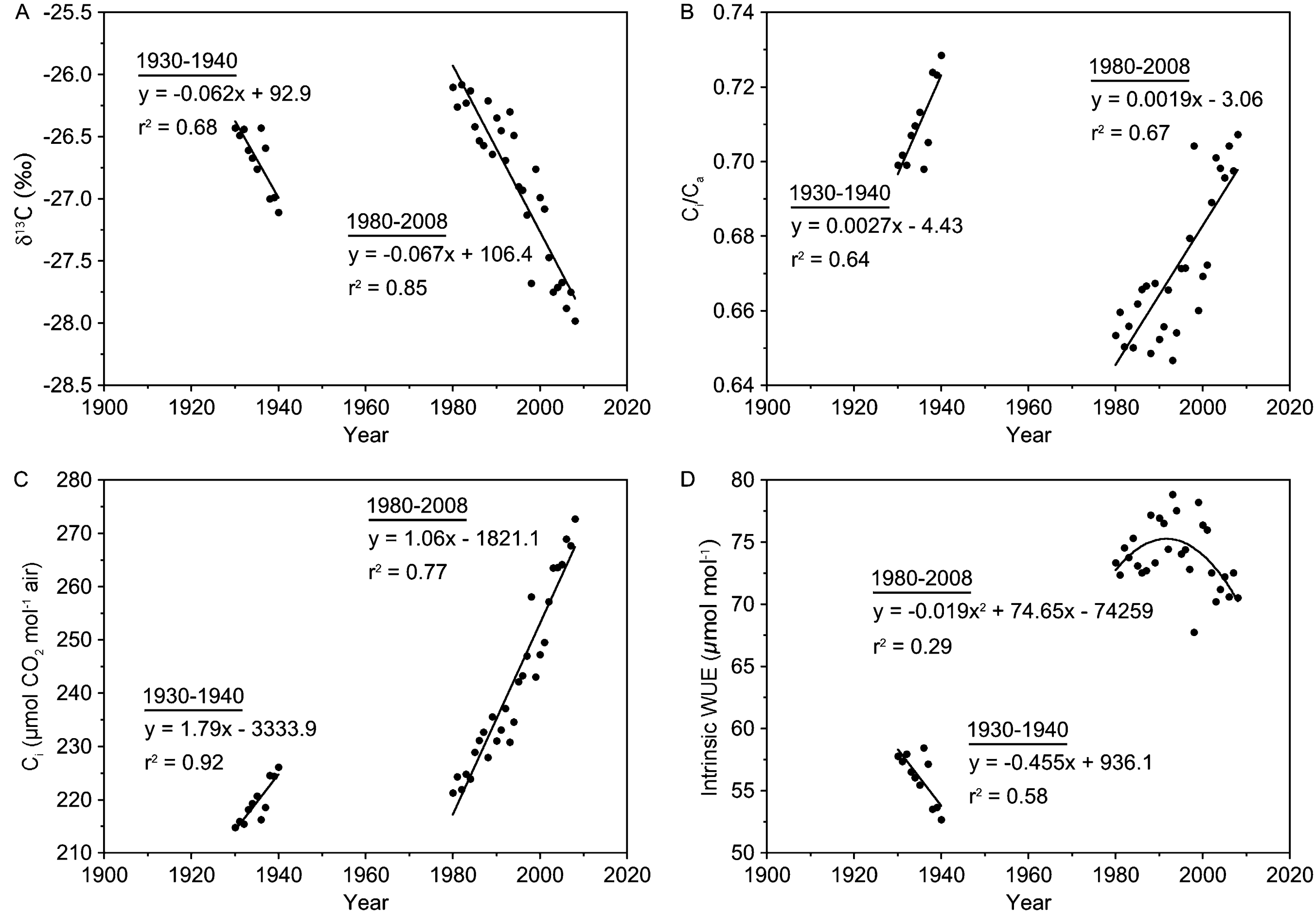

Fig. S5. Comparison of temporal trends of (*A*) $\delta^{13}C$, (*B*) C_i/C_a, (*C*) C_i, and (*D*) intrinsic water-use efficiency (*i*WUE) of *J. virginiana* during 1930–1940 and after 1980.

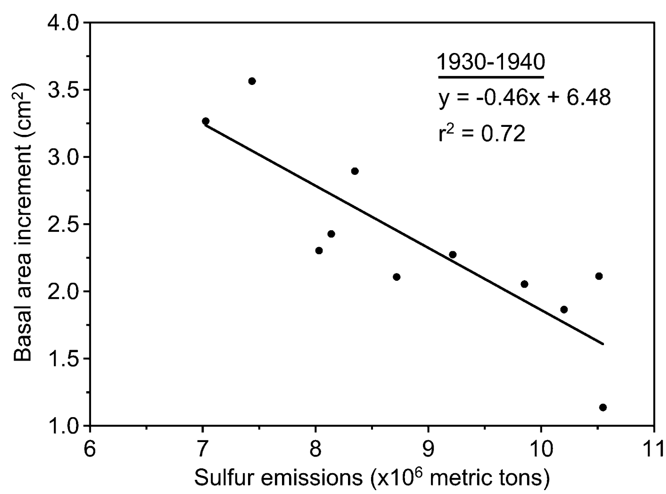

Fig. S6. The relationship between basal area increment of *J. virginiana* with US SO_2 emissions from 1930 to 1940. US SO_2 emissions are taken from ref. 1.

1. Lefohn AS, Husar JD, Husar RB (1999) Estimating historical anthropogenic global sulfur emission patterns for the period 1850-1990. *Atmos Environ* 33(21):3435–3444.

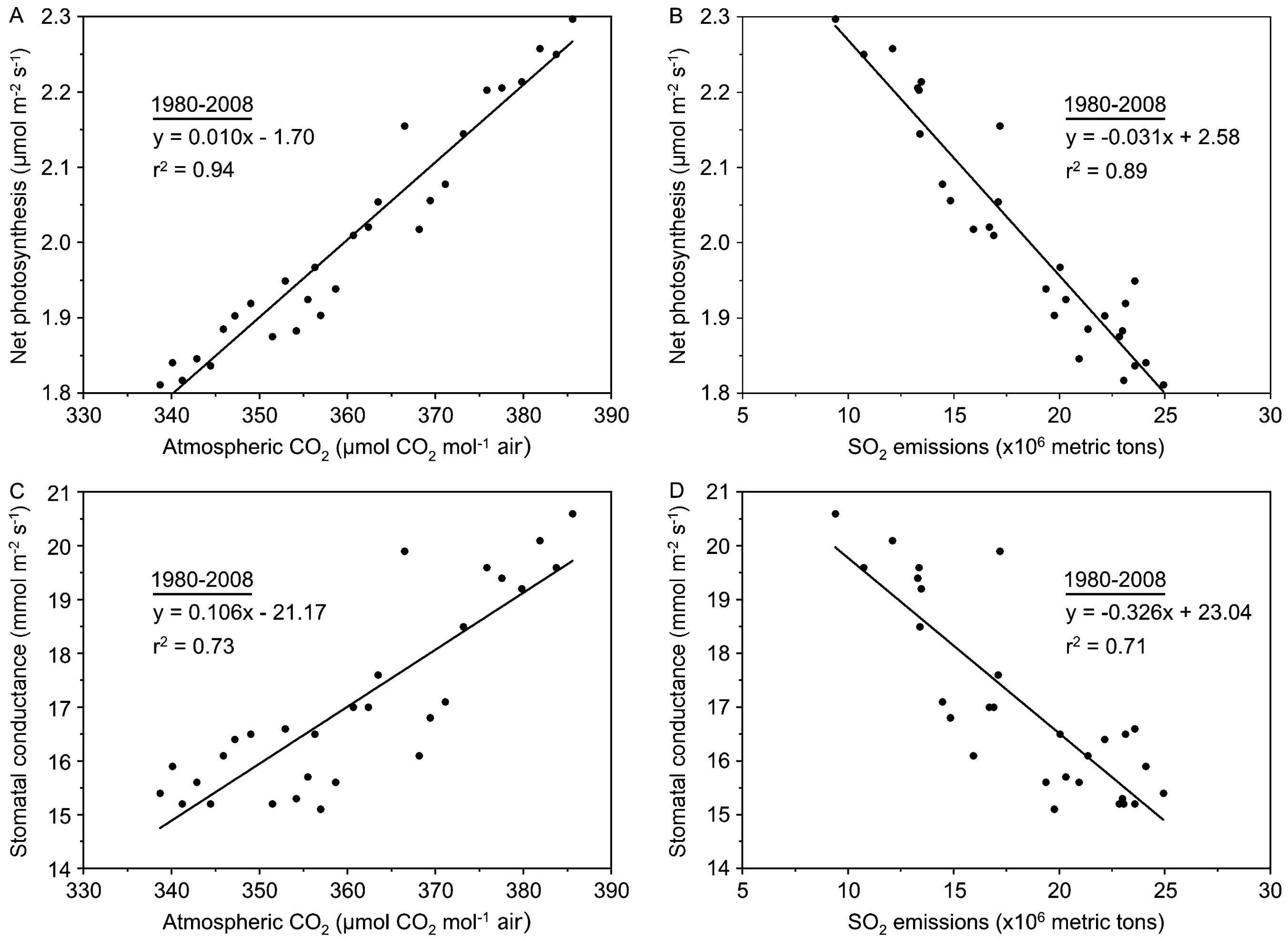

Fig. S7. Relationships after 1980 between simulated seasonally integrated photosynthesis with atmospheric CO_2 concentrations (*A*) and US SO_2 emissions (*B*). Relationships after 1980 between simulated seasonally integrated stomatal conductance to CO_2 with atmospheric CO_2 concentrations (*C*) and US SO_2 emissions (*D*). Atmospheric CO_2 concentrations were taken from (1) and US SO_2 emissions are taken from (2).

1. Keeling RF, Piper SC, Bollenbacher AF, Walker JS (2009) Atmospheric CO_2 records from sites in the SIO air sampling network, in *Trends: A Compendium of Data on Global Change* (Carbon Dioxide Information Analysis Center, Oak Ridge National Laboratory, US Department of Energy, Oak Ridge, TN). Available at http://cdiac.ornl.gov/trends/co2/sio-mlo.html.
2. US Environmental Protection Agency (2012) *National Emissions Inventory (NEI) Air Pollution Emissions* (US Environmental Protection Agency, Chicago). Available at www.epa.gov/ttn/chief/trends/index.html. Accessed September 8, 2012.

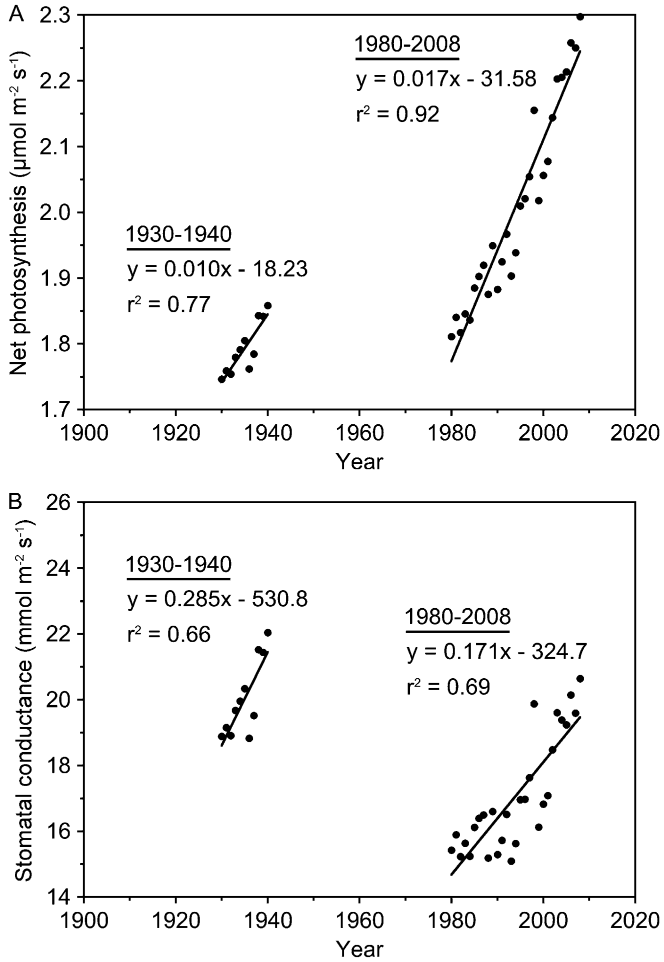

Fig. S8. Comparison of seasonally integrated (*A*) photosynthesis and (*B*) stomatal conductance of *J. virginiana* during 1930–1940 and after 1980.

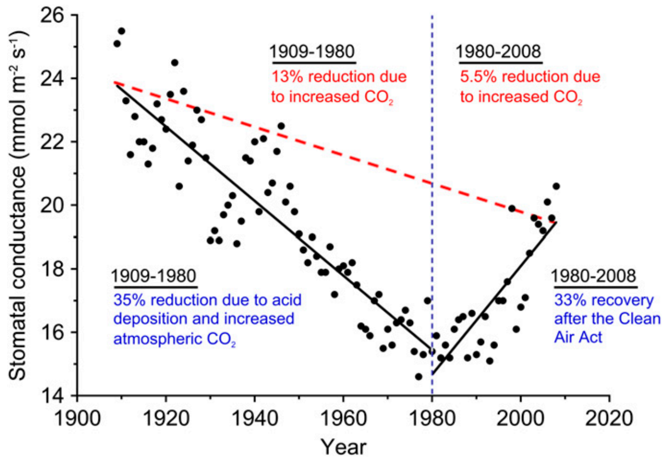

Fig. S9. Changes in stomatal conductance for *J. virginiana* from 1909 to 2008 due to the combined effects of increasing atmospheric CO_2 and acid deposition. Assuming that a complete recovery from acid deposition occurred between 1980 and 2008, the difference in stomatal conductance from 1909 to 2008 reflects the effect of CO_2 (18.5% reduction; dotted red line). Before 1980, the 35% reduction in stomatal conductance is partitioned between a 13% reduction caused by increased CO_2 and a 22% reduction attributable to acid deposition (35–13% = 22%).

Table S1. Correlations between environmental factors and the chronology of *Juniperus virginiana* basal area increment using Kendall's rank correlation analysis

Environmental factor	Kendall's rank correlation coefficient (τ)	Kendall's rank correlation *P* value
CO_2 concentrations	0.7155	<0.0001
NO_x emissions	0.5860	<0.0001
SO_2 emissions	−0.1843	0.0075
Temperature		
Year	0.1584	0.0233
April–August	0.0775	0.2667
Precipitation		
Year	0.1179	0.0871
April–August	0.0610	0.3761
PDSI		
Year	0.1254	0.0692
April–August	0.1309	0.0577